

Supplementary Information for

Improved Radical Stability of Viologen Anolytes in Aqueous Organic Redox Flow Batteries

Bo Hu,^a Yijie Tang,^b Jian Luo,^a Grant Grove,^a Yisong Guo,^b T. Leo Liu^{*a}

^a Department of Chemistry and Biochemistry, Utah State University, Logan, USA

^b Department of Chemistry, Carnegie Mellon University, Pittsburgh, USA

*Corresponding author, E-mail: leo.liu@usu.edu

Experimental details

Materials

2,2,6,6-Tetramethoxy-4-aminopiperidine was purchased from Ark Pharm fine chemicals. Methyl iodide, 4,4'-bipyridine, (3-bromopropyl)trimethylammonium bromide and Amberlite[®] IRA-900 chloride form anion exchange resin were received from Sigma Aldrich. All the chemicals were used as received without further treatment.

Synthesis of active materials

(NPr)₂V, MV, and N^{Me}-TEMPO were synthesized according to literature.^{1,2}

[(NPr)₂V]^{+•} and [MV]^{+•} radicals. Both radicals were prepared in a same manner (described for [(NPr)₂V]^{+•} following). In an Argon or N₂ glovebox (< 0.5 ppm O₂), (NPr)₂V (9.8 mg, 0.03 mmol) was dissolved in 3.0 mL degassed de-ion water in a 10 mL vial, and then Zn powder (4.0 mg, 0.06 mmol) was added into the solution. The reaction solution was monitored by UV-Vis to determine the completion of the reaction. After filtering the excess Zn powder, the obtained 10 mM solution was used for other studies.

Caution: viologen molecules are generally toxic. One should avoid any oral contact when using them in lab.

Radical degradation tests by UV-Vis

In the Argon-filled glovebox, a 0.1 mM radical solution ([[(NPr)₂V]^{+•} or [MV]^{+•}) in 2.0 M NaCl solution was prepared. The solution was added into quartz cuvettes sealed with a Teflon septum. UV-vis spectra were collected every 2 hours for 48 hours to monitor the degradation of the radicals by an Ocean Optical UV-vis spectrometer.

EPR test

Two EPR samples were prepared using the following procedure: All steps were performed in a N₂ glovebox (<0.5 ppm O₂). Deionized H₂O used during the sample preparation was degassed to remove O₂ prior to the experiments. 22.8 mg MV or (NPr)₂V was dissolved in 0.887 ml deionized H₂O, then 3.1 mg fine Zn powder was mixed with the anolyte solution. After mixing, 0.2 ml of the solution was transferred and further diluted with an additional 0.2 ml of deionized H₂O to reach the final volume of 0.4 ml. This final solution was transferred into EPR tube and frozen in liquid nitrogen.

X-band EPR spectra (Fig. S2) were measured on a Bruker Elexsys E-500 spectrometer equipped with an Oxford ESP-910 cryostat. The detailed measurement conditions are temperature 17 K, microwave power 2 μW, modulation amplitude 0.05 mT, modulation frequency 100 kHz, microwave frequency 9.64 GHz. The EPR spectra simulation was performed by SpinCount program. Each spectrum can be fitted with an isotropic g (g_x = g_y = g_z) value. g strain (σ_g, the distribution of g values) was used to account for the broadness of the linewidth.

Electrochemical measurements

All electrochemical CV experiments were carried out in 0.5 M NaCl supporting electrolyte solutions. Cyclic voltammetry experiments were performed with a Gamry 1000E potentiostat. All potentials were referenced to NHE according to the known $MV^{2+/+}$ redox couple (-0.45 V vs NHE). The working electrode (1 mm PEEK-encased glassy carbon, Cypress Systems EE040) was polished using Al_2O_3 (BAS CF-1050, dried at 150 °C under vacuum) suspended in deionized H_2O , then rinsed with deionized H_2O and dried with an air flow. The reference electrode consisted of a silver wire coated with a layer of AgCl and suspended in a solution of 0.5 M KCl electrolyte. A glassy carbon rod (Structure Probe, Inc.) was used as the counter electrode.

Flow battery test

The flow cells for the TEMPO/viologen AORFBs were constructed with two carbon electrolyte chambers, two graphite felt electrodes (SGL Carbon Group, Germany) and a piece of anion exchange membrane sandwiched between graphite felts, and two copper current collectors. Each carbon chamber was connected with an electrolyte reservoir using a piece of Viton tubing. The electrolyte reservoir is home designed and is a 10 mL glass tube. The active area of the cell was 10 cm^2 . A Masterflex® L/S® peristaltic pump (Cole-Parmer, Vernon Hills, IL) was used to press sections of Masterflex tubing to circulate the electrolytes through the electrodes at a flow rate of 60 mL/min. In each reservoir, the balanced flow cell employed 12 mL of the NaCl electrolytes containing 0.5 M active materials. Both reservoirs were purged with nitrogen to remove O_2 and then sealed before cell cycling. The flow cell was galvanostatically charged/discharged at R.T. on a battery tester (LANHE Instruments) in the voltage range of 1.7 – 0.3 V at current densities ranging from 40 to 100 mA/cm^2 . Polarization and EIS experiments were conducted using a Gamry 5000E potentiostat. For the polarization test, the flow battery was first charged at 40 mA/cm^2 and then at 5 mA/cm^2 to achieve 100% SOC (13.4 Ah/L, see Fig. S1).

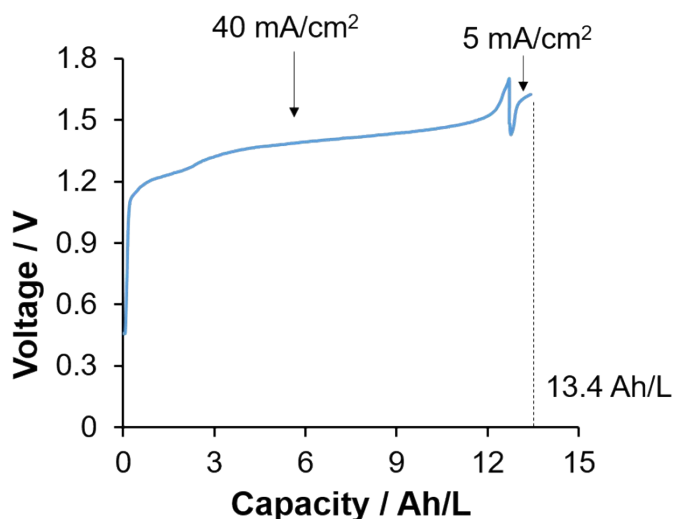


Fig. S1. Capacity vs. voltage profile of the charging process to achieve 100 % SOC. Current density was applied at 40 mA/cm^2 and then 5 mA/cm^2 to achieve 100 % capacity (13.4 Ah/L) of the 0.5 M viologen/TEMPO AORFB for polarization tests.

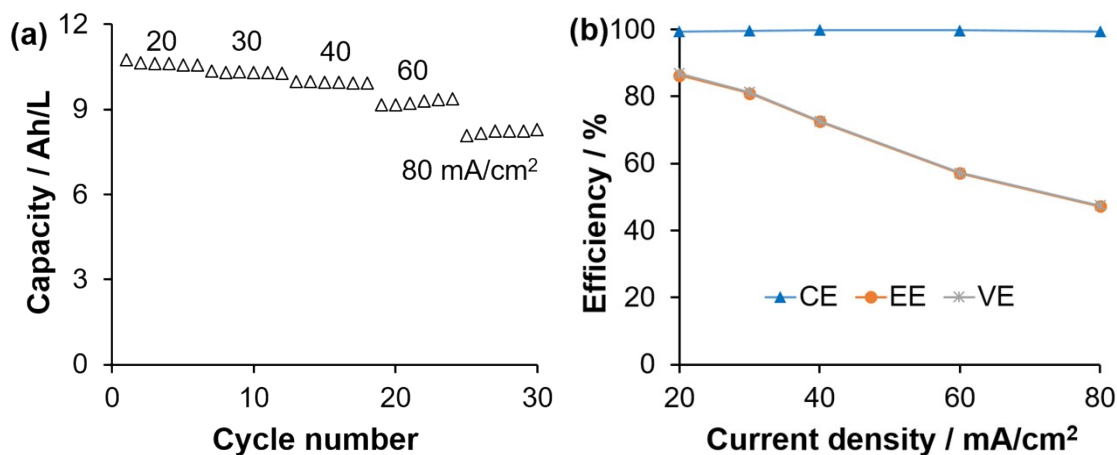


Fig. S2. Battery performance of 0.5 M $(\text{NPr})_2\text{V}/\text{N}^{\text{Me}}\text{-TEMPO}$ AORFB. (a) Rate performance at different charging/discharging current densities. (b) Average coulombic efficiency (CE), voltage efficiency (VE), and energy efficiency (EE) at different charging/discharging current densities.

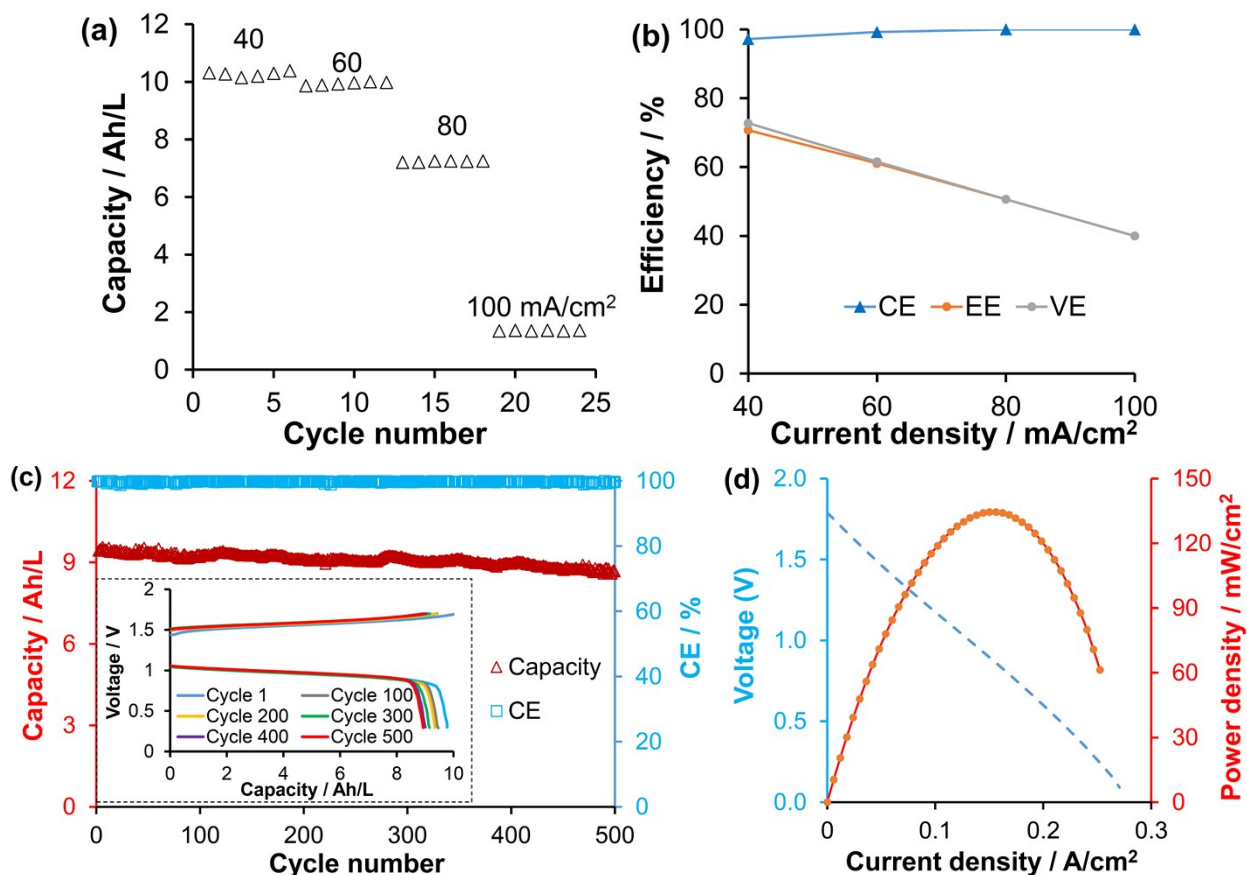


Fig. S3. Battery performance of 0.5 M $\text{MV}/\text{N}^{\text{Me}}\text{-TEMPO}$ AORFB. (a) Rate performance at different charging/discharging current densities. (b) Averaged Coulombic efficiency (CE), voltage efficiency (VE) and energy efficiency (EE) at different charging/discharging current densities. (c) Capacity and CE versus cycle number for 500 cycles. Inserted are the representative voltage versus capacity profiles. The battery was cycled at 60 mA/cm². (d) Polarization curve and power density of the 0.5 M $\text{MV}/\text{N}^{\text{Me}}\text{-TEMPO}$ AORFB.

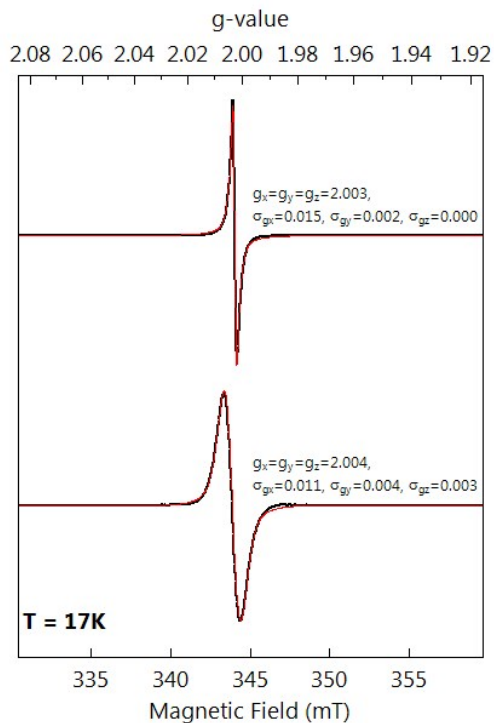


Fig. S4. EPR spectra (black) of $[MV]^{+\bullet}$ (top) and $[(NPr)_2V]^{+\bullet}$ (bottom) and the corresponding spectral simulations (red). The simulation parameters are given in the figure.

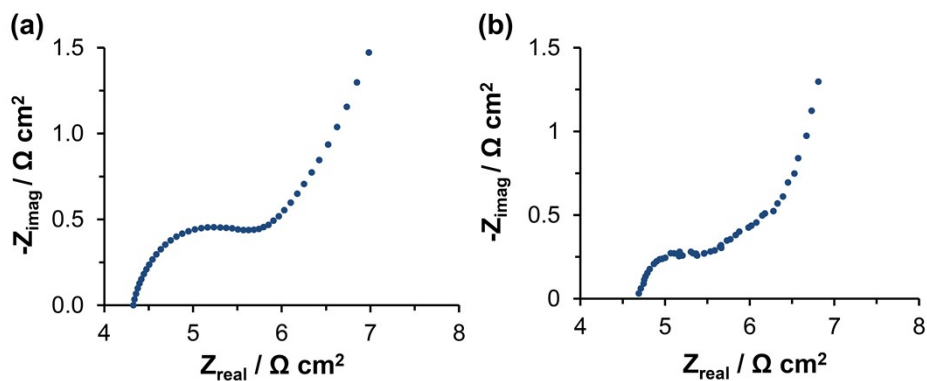
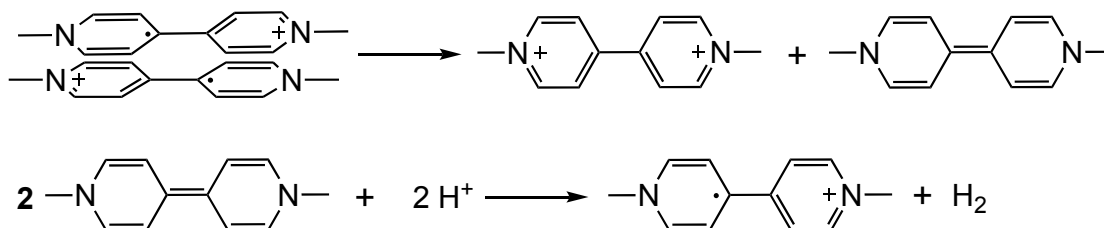
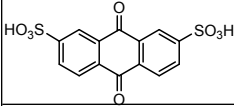
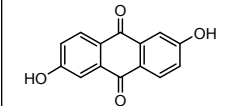
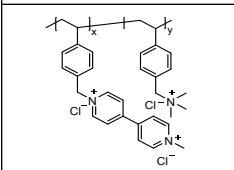
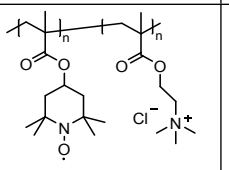
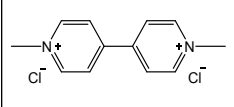
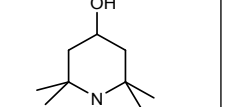
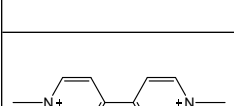
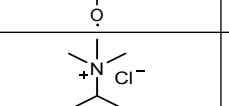
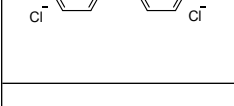
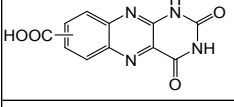
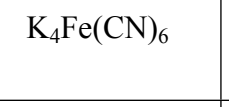
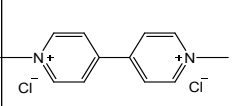
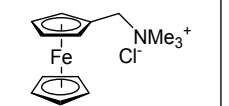
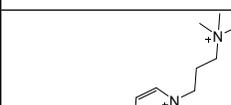
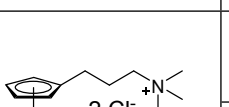


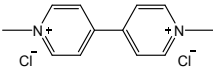
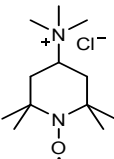
Fig. S5. Nyquist plots of the (a) MV/N^{Mc} -TEMPO AORFB and (b) $(NPr)_2V/N^{Mc}$ -TEMPO AORFB before cycling.



Scheme S1. Proposed reaction mechanism involving the disproportion and proton reduction reactions of methyl viologen radical cations.

Table S1. An overview of representative AORFBs reported to date

Anode	Cathode	Supporting electrolyte	Concentration (M)	Cell voltage (V)	Stability (% per cycle)
	Br ₂	1 M H ₂ SO ₄	1	0.86	99.84 ³ (750 cycles)
	K ₄ Fe(CN) ₆	1 M KOH	0.5	1.2	99.1 ⁴ (100 cycles)
		2 M NaCl	0.373 (based on redox active moiety)	1.15	~99.8 ⁵ (100 cycles)
		1 M NaCl	0.5	1.25	99.89 ⁶ (100 cycles)
		None	2	1.4	99.96 ¹ (100 cycle)
	K ₄ Fe(CN) ₆	1 M KOH	0.5	1.2	99.98 ⁷ (400 cycles)
		2 M NaCl	0.5	1.05	99.987 ⁸ (700 cycles)
		None	0.75	0.75	99.9989 ⁹ (500 cycles)
		None	1.3	0.75	99.9943 (250 cycles)
		2 M NaCl	0.5	1.38	99.995 (500 cycle) (this work)

		2 M NaCl	0.5	1.4	99.982 (500 cycle) (this work)
---	---	----------	-----	-----	--------------------------------------

Reference:

1. T. Janoschka, N. Martin, M. D. Hager and U. S. Schubert, *Angew. Chem. Int. Ed.*, 2016, **55**, 14425-14428.
2. C. DeBruler, B. Hu, J. Moss, X. Liu, J. Luo, Y. Sun and T. L. Liu, *Chem.*, 2017, **3**, 961-978.
3. B. Huskinson, M. P. Marshak, C. Suh, S. Er, M. R. Gerhardt, C. J. Galvin, X. D. Chen, A. Aspuru-Guzik, R. G. Gordon and M. J. Aziz, *Nature.*, 2014, **505**, 195-198.
4. K. X. Lin, Q. Chen, M. R. Gerhardt, L. C. Tong, S. B. Kim, L. Eisenach, A. W. Valle, D. Hardee, R. G. Gordon, M. J. Aziz and M. P. Marshak, *Science.*, 2015, **349**, 1529-1532.
5. T. Janoschka, N. Martin, U. Martin, C. Friebe, S. Morgenstern, H. Hiller, M. D. Hager and U. S. Schubert, *Nature.*, 2015, **527**, 78-81.
6. T. B. Liu, X. L. Wei, Z. M. Nie, V. Sprenkle and W. Wang, *Adv. Energy. Mater.*, 2016, **6**.
7. K. Lin, R. Gómez-Bombarelli, E. S. Beh, L. Tong, Q. Chen, A. Valle, A. Aspuru-Guzik, M. J. Aziz and R. G. Gordon, *Nat. Energy*, **2016**, 1, 16102.
8. B. Hu, C. DeBruler, Z. Rhodes and T. L. Liu, *J. Am. Chem. Soc.*, 2017, **139**, 1207-1214.
9. E. S. Beh, D. De Porcellinis, R. L. Gracia, K. T. Xia, R. G. Gordon and M. J. Aziz, *ACS Energy Lett.*, **2017**, 639-644.